
Optimization of the non-normal incidence, transient pumped plasma X-ray laser for laser spectroscopy and plasma diagnostics at the facility for antiproton and ion research (FAIR)

TH. KUEHL,^{1,2} D. URSESCU,¹ V. BAGNOUD,¹ D. JAVORKOVA,¹ O. ROSMEJ,¹ K. CASSOU,³
S. KAZAMIAS,³ A. KLISNICK,³ D. ROS,³ P. NICKLES,⁴ B. ZIELBAUER,^{1,2,4} J. DUNN,⁵
P. NEUMAYER,^{1,5} G. PERT,⁶ AND THE PHELIX TEAM

¹GSI, Darmstadt, Germany

²University of Mainz, Mainz, Germany

³Université Paris Sud/LIXAM, Paris, France

⁴MBI, Berlin, Germany

⁵Lawrence Livermore National Laboratory, Livermore, California

⁶York University, York, United Kingdom

(RECEIVED 6 October 2006; ACCEPTED 26 October 2006)

Abstract

Intense and stable laser operation with Ni-like Zr and Ag was demonstrated at pump energies between 2 J and 5 J energy from the PHELIX pre-amplifier section. A novel single mirror focusing scheme for the TCE x-ray laser (XRL) has been successfully implemented by the LIXAM/MBI/GSI collaboration under different pump geometries. This shows potential for an extension to shorter XRL wavelength. Generation of high quality XRL beams for XRL spectroscopy of highly charged ions is an important issue within the scientific program of PHELIX. Long range perspective is the study of nuclear properties of radioactive isotopes within the FAIR project.

Keywords: High Power Laser; Laser spectroscopy; Plasma diagnostics; X-ray laser

MOTIVATION

The GSI heavy ion accelerator facility will be extended to the international facility for heavy ion and antiproton research (FAIR) during the next year (Henning, 2004), allowing for a rich field of novel experiments in nuclear and particle physics, atomic physics (Stoehlker *et al.*, 2003), plasma physics (Hoffmann *et al.*, 2005; Schaumann *et al.*, 2005), and applied sciences. An important issue within the scientific program of the PHELIX petawatt high-energy laser (Neumayer *et al.*, 2005) is the generation of X-ray laser beams for advanced diagnostics of plasmas generated by the heavy ion beam, and for XRL spectroscopy of highly charged ions (Neumayer *et al.*, 2001). One of the key features of FAIR will be the ability to generate a wide spectrum of radioactive isotopes throughout the chart of nuclides. Although the information on nuclear ground-state properties extracted

from a study of hyperfine structure and isotope shift is model-independent, it is hampered in complex neutral atoms by the accuracy with which the electron wave functions are known at the site of the nucleus. In that respect, it is highly advantageous to measure these effects in highly charged ions with one or only a few electrons. Since the electron wave function can be precisely calculated in such simple few-electron systems, uncertainties are negligible due to the atomic hyperfine fields at the site of the nucleus. In this way, absolute charge radii can be determined instead of only changes in charge radii between two isotopes of the same element as accessible by conventional isotope shift measurements. In terms of atomic physics, the determination of the specific mass shift given by a comparison of atomic and Li-like isotope shifts provides a means to disentangle features of multi-electron correlation. Li-like ions are a favorable compromise, because here the ground state $2S_{1/2} \rightarrow 2P_{1/2}$ transition is—with the additional help of the large Doppler shift of relativistic ions—in reach for typical XRLs, and the theoretical treatment is possible with high accuracy.

Address correspondence and reprint requests to: Th. Kuehl, GSI, Darmstadt, Germany. E-mail: t.kuehl@gsi.de

The low lying ionic states of Li-like uranium are shown in Figure 1 where the transition energy is 281 eV. This means that the method shown here will be applicable to the entire available range of radioactive isotopes. This possibility is especially important within the projected FAIR facility shown in Figure 2. Here mass separated radioactive isotopes will be available with high beam intensities at the superconducting fragment separator (Super-FRS), and in the next-generation heavy ion storage ring (NESR). Photon energies around 80 eV, as presently achieved at PHELIX will reach well up to lithium-like lead.

EXPERIMENTAL SET-UP OF THE X-RAY LASER

The XRL experiments in Ni-like Zr at PHELIX were performed in two campaigns with similar set-ups. The first one (Neumayer *et al.*, 2004) was using Zr and an incident angle on target of 45° for the main pulse. In a second experimental campaign with Zr, an incidence angle on target of 72° was used (see Fig. 3). The pump beam of 2 to 5 J energy is split into two parts: 75% of the energy are entering in the compressor which re-compresses the pulse down to 400 fs. The transmission of the device is slightly better than 50%. The remaining 25% of the energy are directly transported to the target. In addition to these, a third beamtime used Ag targets and 45° configuration.

The duration of this un-compressed pulse is about 0.8 ns. It is passed through an 18 m long optical delay line in order to produce nearly the same optical path length as the travel

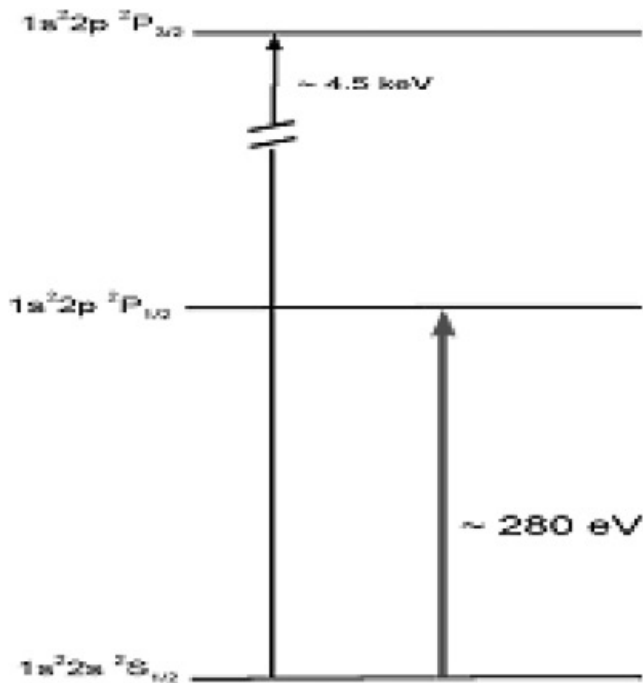


Fig. 1. Level scheme of lithium-like ions with the transition energies for Li-like uranium.

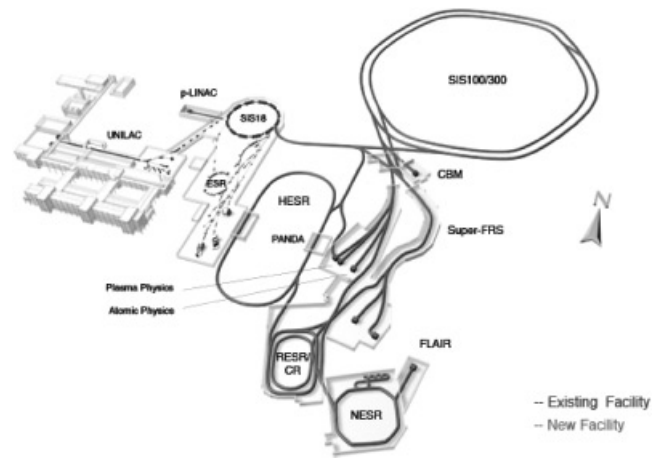


Fig. 2. Aerial view of present GSI with the new FAIR facility additions.

distance in the compressor. This nanosecond pulse is focused by a spherical lens with 1 m focal length, and a cylindrical lens with 250 mm focal length to a line focus of $30 \mu\text{m} \times 6 \text{mm}$ onto a Zr metal target. Here it serves to create a plasma column several hundreds of picoseconds before the impact of the compressed pulse. Due to the ultra-high intensity of the short ps-pulse, this plasma is rapidly heated, which leads to a non-stationary population inversion with a high transient gain. A single, gold coated, 6 in diameter on-axis parabola, tilted at an incidence angle of 9° , is used to generate a line focus of $30\text{--}100 \mu\text{m}$ width and about 5 mm length.

The lifetime of the high gain in the transient collisionally pumped (TCE) scheme is typically in the order of a few picoseconds. Therefore, the focused pulse front of the short pulse creating the population inversion in the plasma has to run along the plasma column with approximately the speed of light c to maximize the overlap of the X-ray pulse and the gain peak. The tilted on-axis parabola intrinsically leads to a tilt of the pulse front generating in this way the “travelling wave excitation” needed for the TCE XRL. The travelling wave speed is $1.4 c$ and $1.1 c$ in the case of 45° and 72° incidence angles on target, respectively.

The properties of the plasma column were further analyzed using an X-ray pinhole camera. This is producing an image of the plasma through a hole of $30 \mu\text{m}$ diameter. A specially designed filter against infrared and visible light ($1 \mu\text{m}$ polypropylene and 200 nm Al) defines the sensitivity range. The magnification of the system is 3.2. The 16 bit camera (Princeton Instruments, Princeton, NJ) used for this purposes, similar to the one for the spectrometer, has a back illuminated cooled $26 \times 26 \text{mm}^2$ chip with 1024×1024 pixels. This allowed to obtain the spatially resolved keV emission image of the whole 4 mm long plasma.

A third camera was installed, monitoring the target in the infrared and visible range. Using adequate motorized filters on a wheel, the visible plasma emission during the shots was monitored. In this way, the overlap of the two infrared

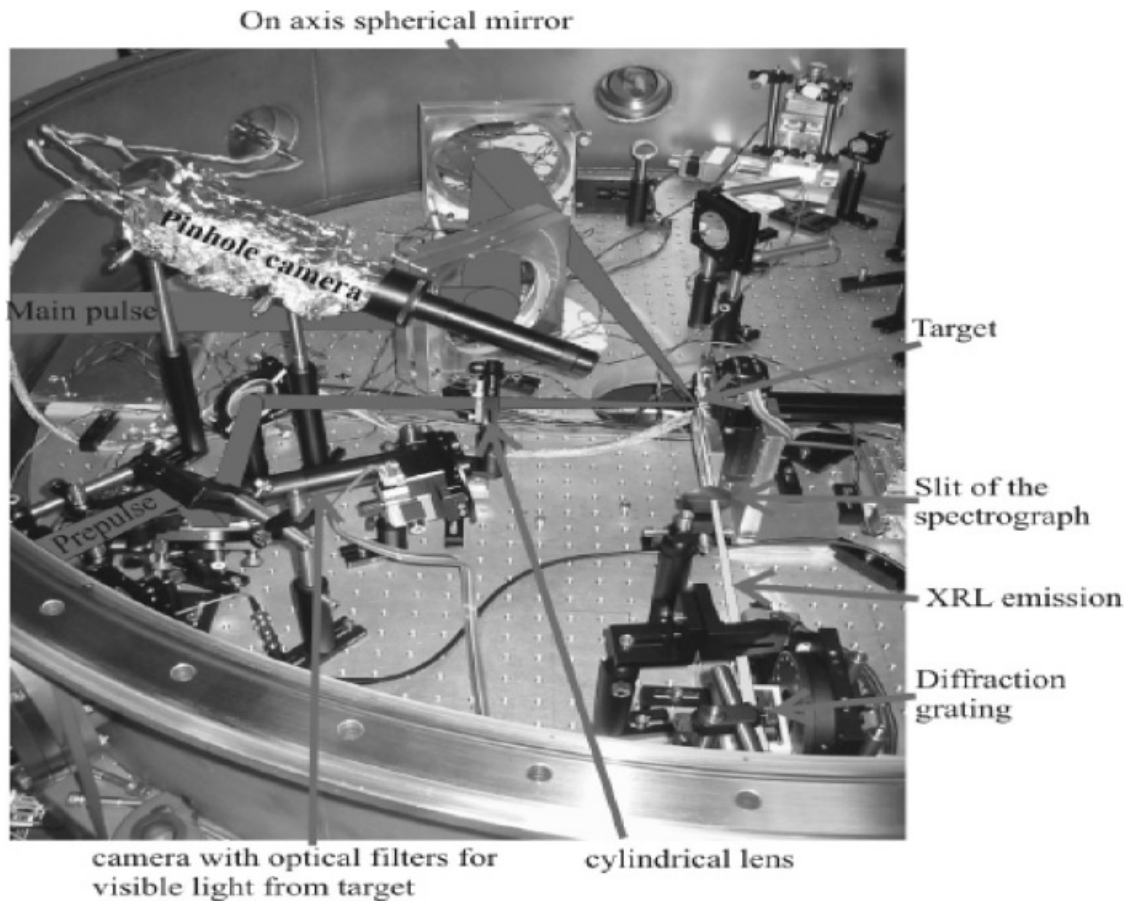


Fig. 3. Experimental set-up with the focusing system for pre-pulse and main pulse, and part of the diagnostics.

pulses along the whole length of the plasma was controlled on-line.

RESULTS

In both geometries, two lasing lines were identified from the emission spectrum of the Ni-like Zr XRL, as shown in

Figure 4. The stronger one at a wavelength of 22.02 nm is identified as the 4d–4p transition and the second one at 26.46 nm as the 4f–4d transition. In both cases, the ratio between the two intensities is about 10. For spectroscopy experiments on Li-like ions, certainly the 22.02 nm lasing line is the better choice. However, the second line might also be important in various situations. For example, if the

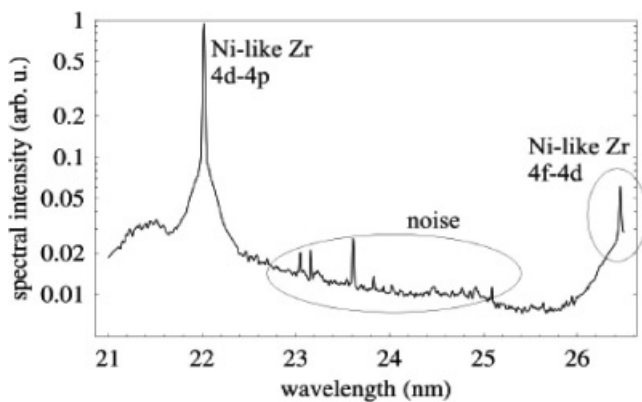


Fig. 4. Logarithmic representation of the obtained lasing lines.

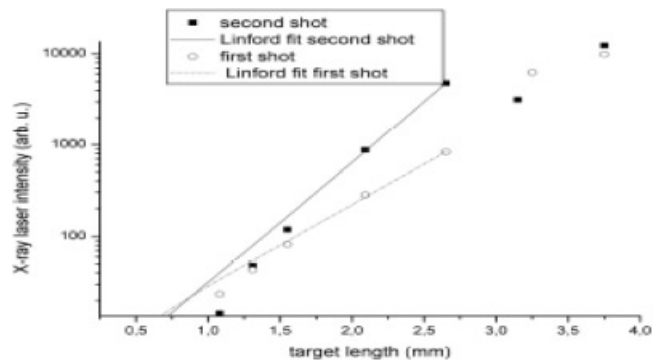


Fig. 5. Gain measurements of the Ni-like Zr X-ray laser depending on the target length. Curves are corresponding to the first and the second shot in one target position. Small gain coefficients of 11/cm and 22/cm were obtained.

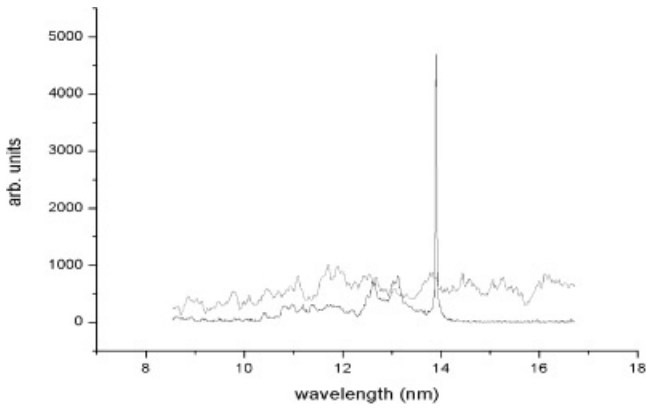


Fig. 6. XRL in Ni-like silver at 13.9 nm.

intensities of the two lasing lines would be equal, due to the beat of the two frequencies, a picosecond long electromagnetic pulse train made of 440 atto-second pulses would be generated. This might be achieved using HHG at 26.4 nm wavelength and injection in a Ni-like Zr XRL.

The gain for the grazing incidence pumping (GRIP) Zr XRL at 22.02 nm was measured at the main pulse duration and peak-to-peak delay where the maximum output was reached. Triangular targets allowed to use plasma lengths from 0.6 mm to 3.8 mm. The results are presented in Figure 5. There were two shots at each position on the target. An interesting clue is provided by the fact that the XRL output intensity from the second shot in one place is systematically higher than the output of first shot in the same place. Fitting individually the first shot series and the second shot series for plasma lengths up to 2.7 mm using the Linford formula, one obtains a small gain coefficient of 11/cm and 22/cm, respectively.

In a very recent experiment, an XRL in Ni-like silver was also demonstrated, as shown in Figure 6. In this case, a total

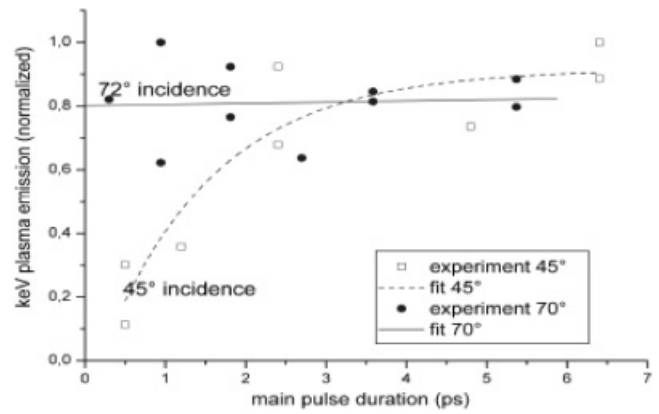


Fig. 8. Comparison of the observed plasma emission for different pulse durations at 45° and 75° incidence angle of the main pulse onto the target. In both cases the plasma emission was detected behind a 500 nm thick aluminium filter, suppressing low energy photons.

pump energy of 5 J was used. Another important parameter can be obtained from Figure 7 where all measurements of the GRIP XRL output as a function of target length are represented in a logarithmic scale. The signature of the saturation for the XRL is given by the roll-off of the curve which appears for target lengths about 3 mm long. This roll-off might be produced by the XRL propagation in plasma, too. In this case, the XRL will be refracted out from the gain region due to the plasma gradients after a distance shorter than the plasma length. This possibility has to be excluded due to the fact that our pre-plasma is produced with a relatively long pre-pulse (800 ps), generating soft plasma gradients, where the refraction index varies slowly. Besides, the length of our plasma medium is below 4 mm. Another argument favoring the interpretation of the saturation roll-off is the gain length product in the order of 10 which is also considered to be a sign for saturation.

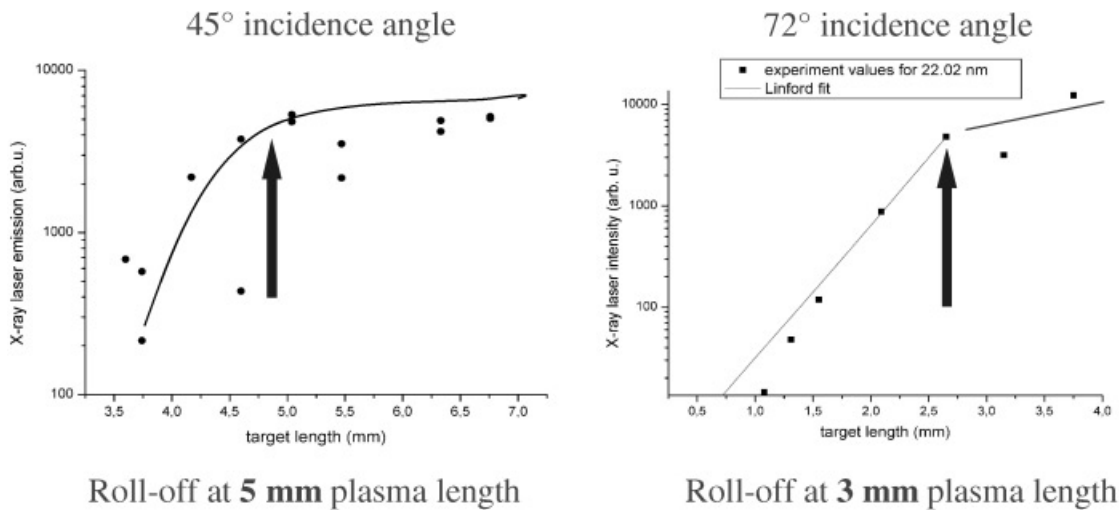


Fig. 7. Measurement of the gain dependence from the target length.

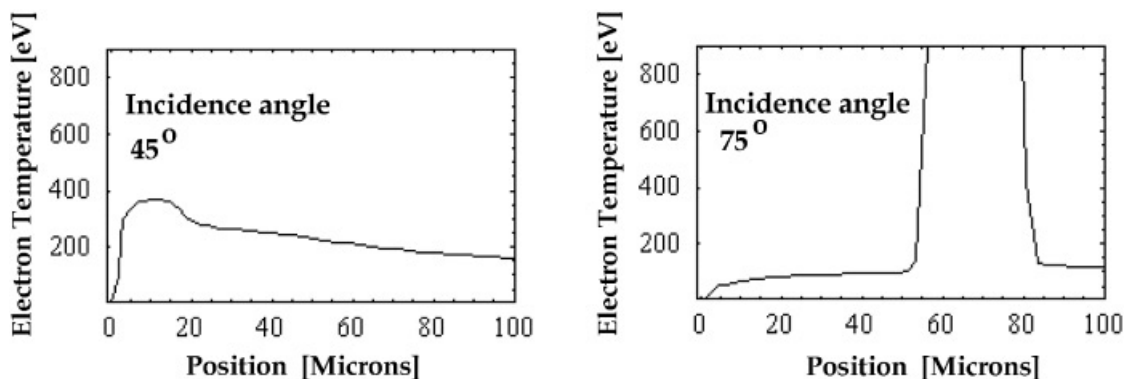


Fig. 9. Electron temperature distribution after heating by the main pulse calculated with the EHYBRID code.

A somewhat surprising result was the strong favoring for shorter main pulse durations at the more grazing incidence angle, as shown in Figure 8. While at 45° incidence angle the plasma emission, detected with a pinhole X-ray camera with an aluminum filter, was rising with increasing pulse duration and showed an optimum between 4 and 5 ps, there was no increase at the 72° configuration. The same behavior was reflected by the laser emission, which showed the maximum at 4 ps and 0.5 ps, respectively. An analysis of the different situations using the EHYBRID code (Pert, 2006) showed good agreement with this behavior. The simulation indicates that the penetration depth at the different angles of incidence leads to a selective heating of very different plasma layers in the two cases, varying strongly in temperature, density, and ionization stage. In Figure 9, the electron temperature distribution reached after heating by the main pulse is shown for 45° and 75° incidence angle. The large difference in the energy deposition is evident. This offers the possibility to select the optimum situation for different pumping conditions, and will be of strong importance for the realisation of shorter wavelength X-ray lasers.

CONCLUSION

Using non-normal incidence pump geometry, we demonstrated gain-saturated soft X-ray lasers at 56 eV and 89 eV photon energy with sufficient pulse energy and beam quality for future spectroscopy experiments, using the sub-10 J output from the PHELIX front-end. This opens the possibility of spectroscopy on Li-like ions in the storage ring. The possibility to tailor the absorption conditions by the choice of the incidence angle of the pump pulse holds promise for the extension of x-ray lasers at moderate pump energy to higher repetition rate (Cassou *et al.*, 2006), and to photon energies beyond 100 eV.

REFERENCES

- CASSOU, K., KAZAMIAS, S., ROS, D., PLE, F., JAMELOT, G., KLISNICK, A., LUNDH, O., LINDAU, F., PERSSON, A., WAHLSTRÖM, C.-G., DE ROSSI, S., JOYEUX, D., ZIELBAUER, B., URSESCU, D. & KUEHL, TH. (2006). Optimization towards high average brightness soft X-ray laser pumped in grazing incidence. *Opt. Lett.* **32**, 139–141.
- HENNING, W.F. (2004). The future GSI facility. *Nucl. Instr. Meth. B* **214**, 211–215.
- HOFFMANN, D.H.H., BLAZEVIC, A., NI, P., ROSMEJ, O., ROTH, M., TAHIR, N., TAUSCHWITZ, A., UDREA, S., VARENTSOV, D., WEYRICH, K. & MARON, Y. (2005). Present and future perspectives for high energy density physics with intense heavy ion and laser beams. *Laser Part. Beams* **23**, 395–395.
- NEUMAYER, P., ALVAREZ, J., BECKER-DE MOS, B., BORNEIS, S., BRUECK, K., GAUL, E.W., HAEFNER, C., JANULEWICZ, K.A., KUEHL, TH., MARX, D., REINHARD, I., TOMASELLI, M., NICKLES, P.V., SANDNER, W. & SEELIG, W. (2001). X-ray laser spectroscopy on lithium-like ions. *Proc. SPIE Int. Soc. Opt. Eng.* **4505**, 236.
- NEUMAYER, P., BOCK, R., BORNEIS, S., BRAMBRINK, E., BRAND, H., CAIRD, J., CAMPBELL, E.M., GAUL, E., GOETTE, S., HAEFNER, C., HAHN, T., HEUCK, H.M., HOFFMANN, D.H.H., JAVORKOVA, D., KLUGE, H.J., KUEHL, TH., KUNZER, S., MERZ, T., ONKELS, E., PERRY, M.D., REEMTS, D., ROTH, M., SAMEK, S., SCHAUMANN, G., SCHRADER, F., SEELIG, W., TAUSCHWITZ, A., THIEL, R., URSESCU, D., WIEWIOR, P., WITTRUCK, U. & ZIELBAUER, B. (2005). Status of PHELIX laser and first experiments. *Laser Part. Beams* **23**, 385.
- NEUMAYER, P., SEELIG, W., CASSOU, K., KLISNICK, A., ROS, D., URSESCU, D., KUEHL, TH., BORNEIS, S., GAUL, E., GEITHNER, W., HAEFNER, C. & WIEWIOR, P. (2004). Transient collisionally excited X-ray laser in nickel-like zirconium pumped with the PHELIX laser facility. *Appl. Phys. B* **78**, 957.
- PERT, G.J. (2006). Optimizing the performance of nickel-like collisionally pumped X-ray lasers. *Phys. Rev. A* **73**, 033809.
- SCHAUMANN, G., SCHOLLMEIER, M.S., RODRIGUEZ-PRIETO, G., BLAZEVIC, A., BRAMBRINK, E., GEISSEL, M., KOROSTIY, S., PIRZADEH, P., ROTH, M., ROSMEJ, F.B., FAENOV, A.Y., PIKUZ, T.A., TSIGUTKIN, K., MARON, Y., TAHIR, N.A. & HOFFMANN, D.H.H. (2005). High energy heavy ion jets emerging from laser plasma generated by long pulse laser beams from the NHELIX laser system at GSI. *Laser Part. Beams* **23**, 503–512.
- STOEHLKER, T., BACKE, H., BEYER, H., BOSCH, F., BRAEUNING-DEMIAN, A., HAGMAN, S., IONESCU, D., JUNGSMANN, K., KLUGE, H.-J., KOZHUHAROV, C., KUEHL, TH., LISEN, D., MANN, R., MOKLER, P. & QUINT, W. (2003). Status and perspectives of atomic physics research at GSI: The new GSI accelerator project. *Nucl. Instr. Meth. B* **205**, 156.